ICAS 2021 SHANG HAI
32nd Congress of the International Council of the Aeronautical Sciences
September 6-10, 2021
Pudong Shangri-La, Shanghai, China

AIRCRAFT ENGINE ROTOR DYNAMICS ANALYSIS AFTER FAN BLADE-OUT WITH ACCOUNT OF ROTOR-CASING CONTACT INTERACTIONS

V. Y. Myasnikov[1], I. I. Ivanov[1], B. S. Blinnik[1]

[1]Dynamics and strength of aviation engines department, Central Institute of Aviation Motors, 111116 Aviamotornaya Street 2, Moscow, Russian Federation

Abstract

The paper presents a simple and efficient approach to modeling the dynamics of the rotor-casing system of an aircraft engine in case of fan blade-out. The proposed method makes it possible to take into account the instantaneous occurrence of a rotor unbalance, a change in the rotational speed due to the rotor-casing contact interaction and aerodynamic forces, the passage of the resonance mode during rotor deceleration. The interactions of the lost blade with the casing and trailing blades are neglected. Special attention is paid to modeling the contact interaction taking into account the flexibility of the blades crown. The comparison of the modeling results using the developed method and detailed three-dimensional modeling are presented. The estimation of the error in determining the maximum loads transmitted from the rotor to the casings are presented.

Keywords: fan blade-out, rotor dynamics, unbalance, rotor-casing interaction, blade rubbing

1. Introduction

Aviation gas turbine engine (GTE) rotor blades are subjected to significant operational loads. The possibility of foreign objects getting into the engine air intake further complicate their work environment. Right now, it is yet impossible to completely eliminate the possibility of blade breakage. Fan blade-out (FBO) consequences can be catastrophic. FBO is detected by the engine control system, the fuel supply is cut off, the rotor speed drops due to contact interactions and aerodynamic forces. A significant increase in structural frame loads occurs in the first moments after the FBO as the broken blade hits the casing and significant imbalance of the low-pressure (LP) rotor emerges almost instantaneously. Even greater loads can take place when passing the resonant modes as the rotor decelerates.

In accordance with the regulatory documents [1, 2], the aircraft should not experience dangerous consequences in case of FBO. Lack of such consequences is confirmed experimentally. The cost of FBO engine tests is extremely high. Engine designers are keen to get through successfully on the first try. Besides that, the FBO loads turn out to be the highest for many engine components and should be known at the design stage. For these reasons developing sufficiently accurate methods of modeling engine FBO dynamics highly important.

Research works on modeling the engine fan blade-out dynamics can be divided into two groups, depending on the factors that contribute to load increase. The first group deal with impact dynamics. The focus of attention is on modeling the interaction of a broken blade with the casing and remaining blades of the fan impeller. The main goal in such works is to estimate the casing ability to contain the broken blade. Modern works of this category typically perform modeling based on explicit time integration of the equations of motion with the use of commercial finite element analysis programs. Plasticity and strain rate dependent mechanical properties are generally taken into account. An example of such works is [3-5].

The authors of [3] provided a detailed FBO simulation in a system consisting of half of the fan casing and a rotor sector with 6 blades – the breaking one, two preceding and three following it. Particular attention is paid to fracture propagation in the blade root. The fracture growth process is modeled by means of sequential removal of elements.

The work [4] investigates the response to the first compressor stage blade-out of a system consisting of a rotor with three full stages of working blades and a casing. Circular and longitudinal flanges of the casing has been considered while taking into account bolt pretention and the possibility of bolt breakage. The maximum casing deflection obtained experimentally and analytically have been compared.

The work [5] attempts to take account of loads caused by both the blade impact and sudden unbalance of the LP rotor. The calculation model includes the full LP rotor mounted on three linear elastic supports, the fan blades and the casing. The motion equation integration interval was 0.1 sec. Numerical investigation of the fan blade-out in the system including all elements of the engine structural frame was performed in [6-8].

In the works of the second group, the focus of the researchers is on determining the system response to the sudden rotor unbalance and passing the resonant mode with variable rotor speed. These problems can be classified as rotor dynamics problems. The unbalanced rotor dynamics behavior have been studied for several decades.

The work [9], for example, builds a nonlinear model to take into account the variable rotational speed, differences in the supports stiffness in mutually perpendicular directions, unequal shaft stiffness in different planes, large deflections, asymmetry of inertial properties of the disk and even nonlinear effects in the supports. The work explores the rotor going through the critical speed and the influence of nonlinear effects on the dynamic process characteristics. The work [10] builds a beam model of the rotor with overhung disk. It analyzes a transient process during rotor deceleration and going through the critical speed. It also evaluates the influence of the gyroscopic effect and the additive equation of motion components related to the variable rotational frequency on the system dynamics. The recent work [11] studies the rotor response to the sudden unbalance in the sub- and supercritical modes both experimentally and analytically.

The FBO response study in a twin-shaft system with an intershaft bearing was performed in [12] on the basis of detailed finite-element modeling. Special attention is paid to asymmetrical inertia characteristics of the fan disk after blade loss and, as a consequence, a possible parametric instability. The extensive review [13] looks at in detail and classifies various approaches to rotor-casing rubbing modeling. Loads on the elements of the engine structure caused by the combined action of all factors can be determined analytically in the simulation using the implicit-explicit approach first proposed in the work [14], also outlined in [15].

This paper presents an approach to the rotor-casing system dynamics modeling under sudden unbalance associated with the blade-out. Particular attention is paid to modeling of the rotor-casing interaction through the blades crown. Basic principles and relations of the proposed method are given in the next section of the paper. Section 3 is devoted to the description of the calculation models, section 4 presents the results of calculations and a comparison of the data obtained by detailed three-dimensional FE modeling and calculations using the proposed approach. The last section contains final remarks and comments.

2. Rotor-casing system dynamic modeling in case of fan blade-out

2.1 Modeling approach

An approach to the analysis of the dynamics of the rotor-casing system of an aircraft GTE taking into account the contact interaction and rotor deceleration was proposed by the authors in [16] and briefly outlined below.

Rotor-casing dynamic response to instantaneous unbalance after FBO is analyzed in time domain by means of integration of the equations of motion (1). To account possible changes in rotor speed due to contact interactions or aerodynamic forces, system is extended by the equation of rotor movement around its axis as a rigid body (1b).

$$\begin{cases} [M]\{\ddot{q}\} + [D]\{\dot{q}\} + \dot{\varphi}[G]\{\dot{q}\} + ([K], \ddot{\varphi}[C])\{q\} = \{f\} & \text{(a)} \\ J_p\ddot{\varphi} = M & \text{(b)} \end{cases} \quad (1)$$

Here $[M], [D], \dot{\varphi}[G], [K], \ddot{\varphi}[C]$ – mass, dissipation, gyroscopic, stiffness and circulation matrices respectively. $\{q\}$ and $\{f\}$ – vectors of generalized degrees of freedom and time-varying loads. J_p – polar moment of inertia of the rotor. M – moment of external forces.

The rotor rotation angle φ, rotation frequency $\dot{\varphi}$ and angular acceleration $\ddot{\varphi}$ are included in the column vectors of displacements $\{q\}$, velocities $\{\dot{q}\}$ ◘ accelerations $\{\ddot{q}\}$ respectively. Thus, the dimension of system (1) is increased by one. Equations (1) are integrated together using the Newmarks method with a constant step. Condition (2) is checked at every time step.

$$\delta = r_o - \Delta > 0 \quad (2)$$

Here r_o – is radial displacement of the rotor in a plane where contact interaction occurs, Δ is initial gap, δ is radial penetration of fan blades' crown inside the casing. In case of gap is closed $\delta > 0$ contact forces are added to the right part of the system (1). Otherwise, contact forces are equal to zero. Normal and tangential components of the contact forces are calculated as follows:

$$\begin{gathered} F_n^{cont} = F_n^{cont}(\delta) \\ F_\tau^{cont} = \mu F_n^{cont} \\ M^{cont} = -sgn(V_A^\tau) F_\tau^{cont}(r_{blade} + \Delta - r_o) \end{gathered} \quad (3)$$

Here r_{blade} is the distance from the rotation axis to the most distant point at the periphery of the fan impeller. V_A^τ – the tangential speed component of this point. V_A^τ is also used in calculation of orthogonal projections F_y^{cont}, F_z^{cont} of the contact forces [16].

Moment of external forces is calculated as follows:

$$M = \begin{cases} M^{aero}(\omega, V), \ r_o < \Delta \\ M^{aero}(\omega, V) - sgn(V_A^\tau) F_\tau^{cont}(r_{blade} + \Delta - r_o), \ r_0 \geq \Delta \end{cases} \quad (4)$$

Here ω – rotor speed, V – forward speed of the aircraft, $M^{res}(\omega, V)$ – moment of aerodynamic forces. $M^{res}(\omega, V)$ is considered a known function that can be determined experimentally. In this paper, for simplicity, we assume $M^{res}(\omega, V) \equiv 0$.

Proposed approach was implemented in a developed software based on a C++ code. Correctness of the implementation and the adequacy of the approach were verified by comparison of results with those computed using MSC Nastran [16].

2.2 Blades crown compliance determination

When the rotor contacts the casing through the blades crown, the latter imposes additional constraint on the rotor and also transmits the load. The blades crown can be considered an additional elastic support with a non-linear characteristic. Changing this elastic characteristic can lead to changes of rotor resonant frequencies and significantly influence the system dynamics.

The blades' compliance is taken into account when modeling the contact interaction by assigning elastic characteristic of the crown as a dependence $F_n^{cont}(\delta)$ in expressions (4). The crown elastic characteristic must be determined by solving a separate problem before integrating equations of motion (1). The elastic characteristic of one blade is obtained from the solution of the contact problem of a blade compression against the absolutely stiff casing. In this case the blade root section is given a radial displacement. The dependence of radial contact force on the casing from the blade root displacement is used as an elastic characteristic. The diagram of the fan blade compression problem and the elastic characteristic obtained from the solution are shown in Fig. 1. The sharp bend in the blade elastic characteristic corresponds to blade buckling.

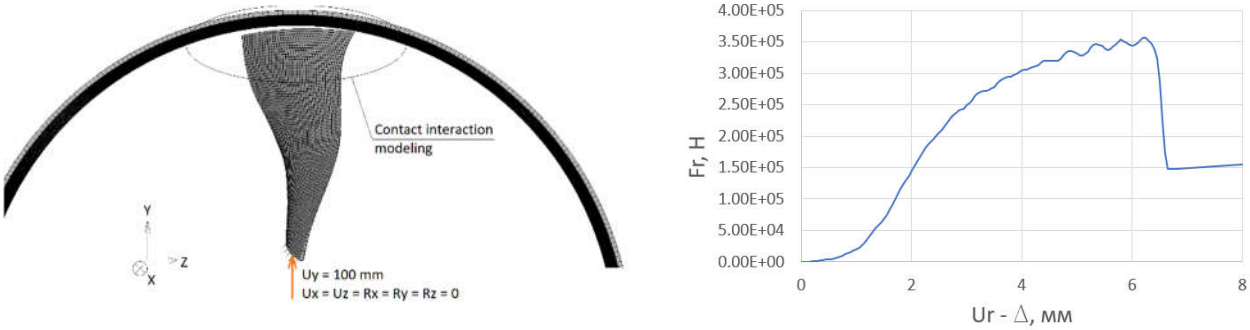

a – diagram of the problem b – blades elastic characteristic

Figure 1 – Determination of the blades elastic characteristic

Centrifugal forces can significantly influence the blade elastic characteristic. Blade stiffening due to centrifugal forces can be taken into account by loading the blade with corresponding forces before compression. Centrifugal load is kept during compression. Fig. 2 shows comparison of the blade elastic characteristic with and without the centrifugal load. Besides increase of blade stiffness due to centrifugal forces elastic characteristics is also can be significantly affected by the blade tip radial displacement and corresponding changes in contact conditions.

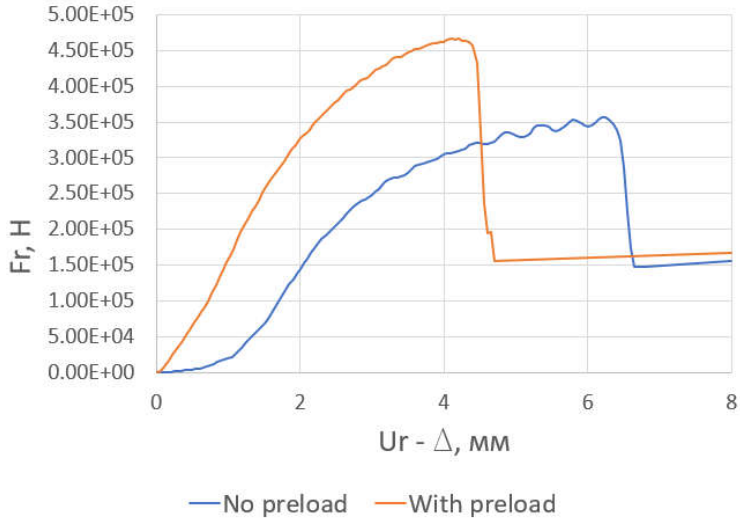

Figure 2 – Influence of centrifugal load on the elastic characteristic of the blade

The crown elastic characteristic can be obtained from the elastic characteristic of one blade, assuming that it behaves as a system of radially oriented springs, with each having the characteristics of a blade. Fig. 3 shows an example of the crown elastic characteristic obtained in this way. The elastic characteristic is calculated for a case of 18 blades in a crown and a 7-mm radial gap. Sharp bends correspond only to the blade buckling but also to the beginning of contact with the neighboring blades.

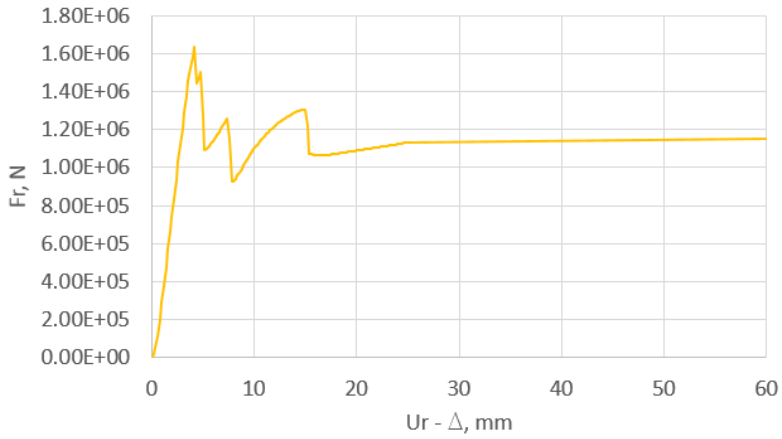

Figure 3 – Elastic characteristic of the blades crown, Δ= 7 mm

Radial gaps between compressor and turbine impeller blades and casings in modern engines are rather small. The gap between the fan blades and the metal part of the casing, however, can exceed 10-15 mm. The space between the blade tip and rigid part of the fan casing is typically filled with a highly flexible noise-absorbing structure and abradable coating. These elements get separated from the casing in the first moments after the FBO and have little effect on the system dynamics. The present work does not take their presence into account.

The considerable gap between the fan blades and the casing significantly influences the elastic characteristic of the blades crown. The overhung fan disk turns out of plane when shifted by rotor unbalance. As a result, there is a change in the blades to casing contact conditions. In order to take this effect into account when determining the elastic characteristic, the blade root section is assigned not only a radial displacement, but also a rotation. The relationship between the radial displacement and rotation is determined by the rotor geometry and support stiffness.

Another factor affecting the blades elastic characteristic is a contact friction. In order to take it into account, the casing can be rotated in the direction opposite to the rotor rotation while compressing the blade. In this case the problem of blade compression against the casing is solved as a dynamics problem. Fig. 4 shows the diagram for determining the blade elastic characteristic taking into account the fan disk out of plane rotation and contact friction.

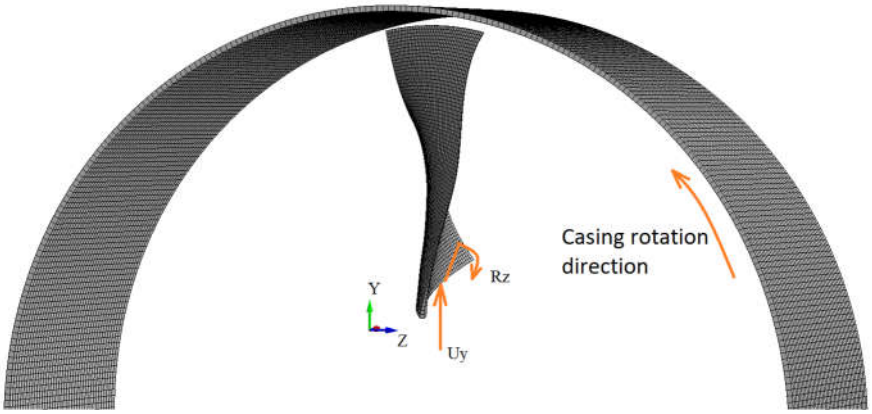

Figure 4 – Determination of the elastic characteristic of the blade in the case of friction and disks out of the plane rotation.

Fig. 5 shows the comparison of the blades crown elastic characteristic, obtained by taking into account out of plane rotation and contact friction.

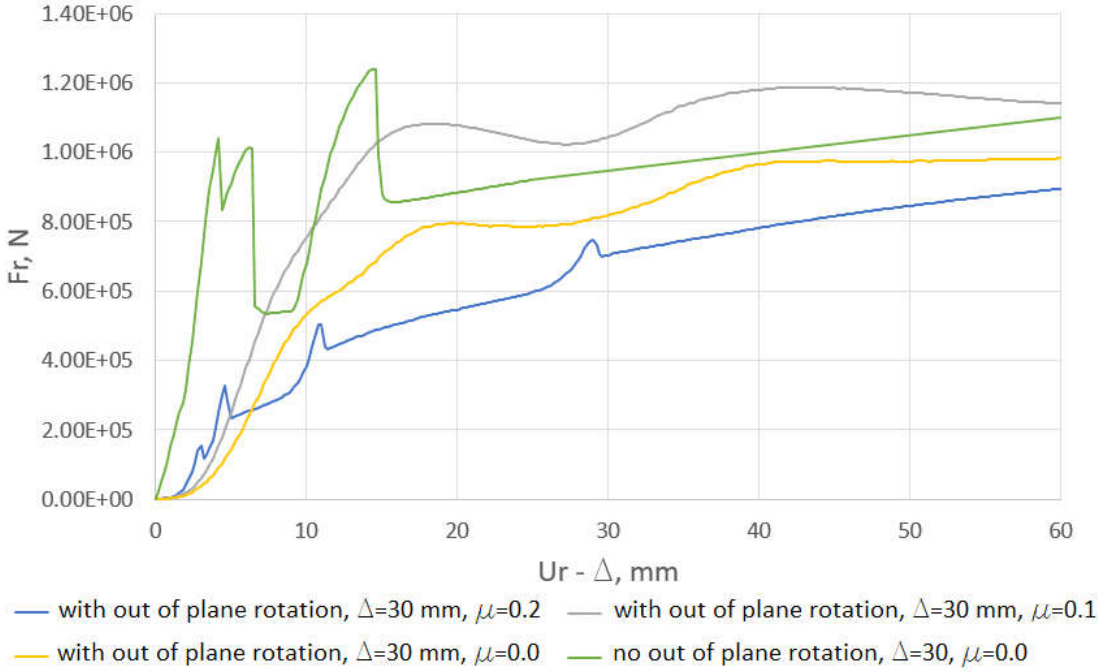

Figure 5 – Blades crown elastic characteristics for different calculation cases

When the disk out of plane rotation is taken into account, the blades crown turns out to be more compliant. This is mainly due to changes in the contact conditions. At compression without out of plane rotation, almost the entire upper edge of the blade comes into contact at once. When disk out of plane rotation is taken into account, only the front part of the blade is in contact.

The contact friction, in its turn, has an ambiguous effect. The curve corresponding to the friction coefficient $\mu = 0.1$ in Fig. 5 goes higher than the curve corresponding to frictionless compression. At this friction coefficient value, the blades crown turns out to have greater stiffness. It can be explained as follows: at frictionless blade compression against the casing the blade buckles and its upper part slips by the casing and bends in the direction of rotor rotation (Fig. 6a); at compression with friction coefficient $\mu = 0.1$ there are no observable differences in the character of the blade deformation. However, as the friction coefficient increases to the value of $\mu = 0.2$, the blades crown becomes more compliant (blue curve in Fig. 5). The reason is differences in the deformed blade configuration after buckling. At $\mu = 0.2$ after the blade buckles the peripheral part does not bend in the direction the rotor rotation, but in the opposite direction (Fig. 6b).

a – $\mu = 0$ and $\mu = 0.1$ b – $\mu = 0.2$

Figure 6 – Blade deformed configuration after buckling

3. Designing the computational model

A series of calculations was carried out to determine the rotor-casing system response to sudden unbalance associated with the fan blade-out in order to assess the accuracy of the results obtained by simulation using the approach outlined in Section 2. Three-dimensional geometric and finite-element models of the rotor-casing system were developed for the calculations. The system parameters are close to the real design of modern civil aviation engines. The model includes a LP rotor mounted on three supports and carrying a fan blades crown, as well as a slightly tapered fan casing. The rotor supports were considered linear-elastic. Their stiffness was assigned accounting the stiffness of the engine casings system, elastic elements and ball or roller bearings themselves. The fan casing was regarded as absolutely rigid and unable to move as a rigid body. The system under study is shown in Fig. 7.

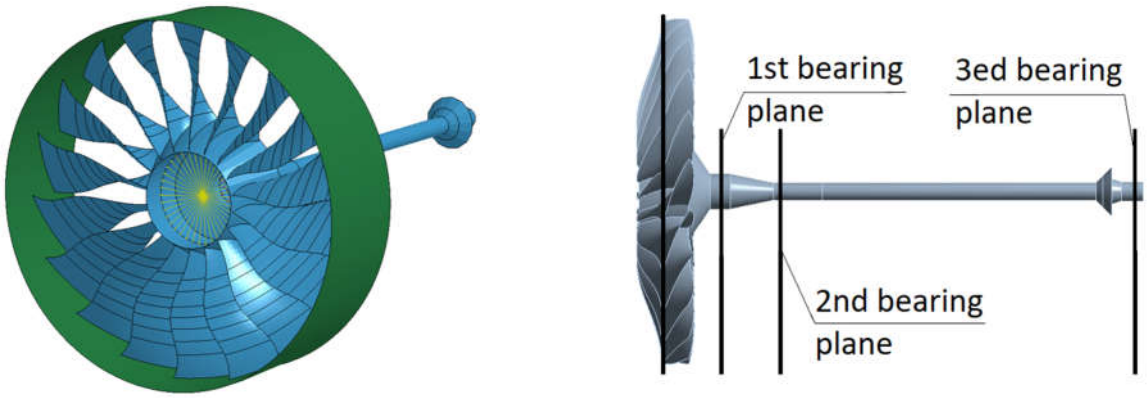

a – isometric view b – bearings location

Figure 7 – Rotor-casing model

3.1 Three-dimensional rotor-casing finite element model

The three-dimensional finite element model of the rotor was created using four-node shell elements. Eight-node solid elements are used for discretization of the blades and casing. Blades to rotor disk connection was modeled in a simplified fashion by creating continuous contact between the lower part of each blade and the outer surface of the disk. This connection is organized in such a way that not only translational motions, but also rotations of the normal are conjoint at the blade-disk junction.

The rotor model contains 1997 elements and 2020 nodes, the casing model contains 39,832 nodes. Three elements across the blade thickness were used. The model of one blade contains 10,650 nodes, the model of the whole crown – 191,700. As a whole, the three-dimensional finite element model of the rotor-casing system consists of 231,552 nodes. Its images are shown in Fig. 8.

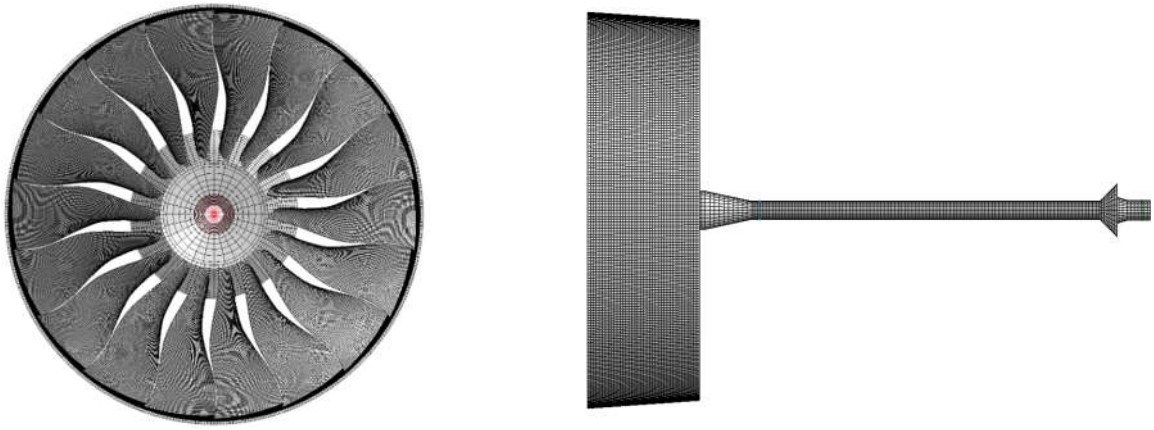

a – front view b – side view

Figure 8 – 3D FE model of the rotor-casing system

The rotor supports are modeled by linear two-node elastic elements. To accommodate such elements, the rotor shell FE model nodes, situated in the support axial plane, are connected by a RBE2-type link with a node on the rotor rotation axis. This node is connected by an elastic element to a coincident at the initial moment of time node. All second node degrees of freedom are constrained. Supports' stiffness, normalized with respect to the maximum value, are given in the Table 1.

Table 1. Normalized rotor bearings stiffness

Support by count from the fan	Stiffness, normalized to the maximum bearing stiffness
1st	0,58
2nd	1,00
3ed	0,35

During modeling, the fan casing was regarded as absolutely rigid and having no possibility of rigid body displacements. Thus, the casing nodes degrees of freedom were not directly taken into account in solving the problem. Casing discretization using a sufficiently fine mesh was carried out in order to correctly account for the contact interaction. The 3D FE model of the system has approximately 580,000 degrees of freedom.

3.2 Model for calculations using the developed approach

The model was changed for modeling using the developed approach. The fan casing is excluded, the blades crown is replaced by a point element with appropriate mass and moments of inertia. This element is placed in the node on the rotor rotation axis in the rotor center of mass plane and is connected to disk nodes through RBE3 link. The model is reduced based on the Guyan method [17] to a number of condensation nodes. Condensation nodes lie on the rotation axis and connected to the nodes of the rotor 3D FE model through RBE2 links for the nodes in the support planes and RBE3 links in other axial planes. The supports are modeled by two-node linear elastic elements similar to the original model. The modified rotor model is shown in Fig. 9, RBE2 and RBE3 links are shown with red lines. 14 condensation nodes were used, so the reduced rotor model matrices used in calculations using the developed approach have dimension of 84x84.

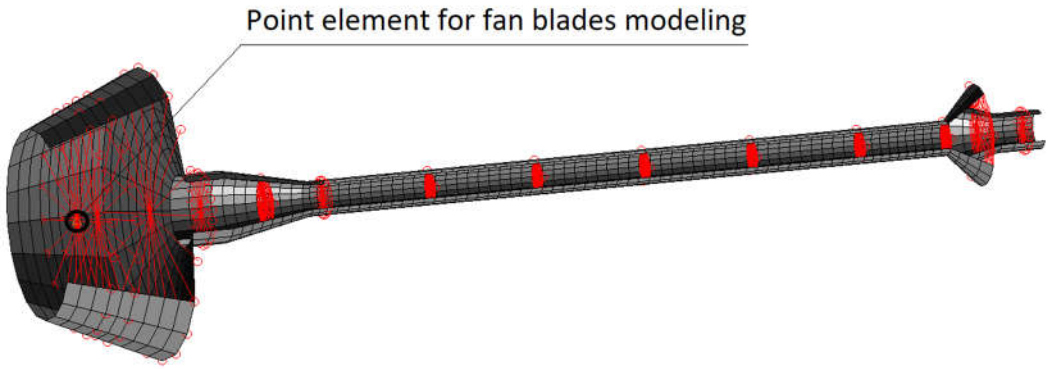

Figure 9 – Modified rotor model for the calculations using proposed approach (before reduction)

Quality of the model obtained through the reduction method depends on the choice of condensation nodes and is subject to evaluation. This evaluation is based on the comparison of natural frequencies of free rotor determined using full and reduced models. Table 2 shows the results of the comparison.

Table 2. Natural frequencies of the free rotor

Mode shape	Frequency of the free rotor, Hz		Error, %
	Full model	Reduced model	
1st bending	32.4	32.4	0.003
2nd bending	92.9	92.9	0.019
3ed bending	239.8	239.5	0.155
1st tortional	259.2	259.1	0.039
1st longitudinal	337.9	337.6	0.092
4th bending	473.4	470.8	0.556
5th bending	774.1	764.4	1.266
2nd tortional	933.9	924.3	1.035
2nd longitudinal	1009.8	1000.1	0.970
6th bending	1136.9	1112.0	2.239

The error does not exceed 2.3% even when determining the higher frequency modes. Table 2 presents data indicating the possibility of using the reduced rotor model to analyze the dynamics of the rotor-casing system without significantly accuracy loss.

4. Rotor-casing dynamics modeling and the results

The dynamics problem was firstly solved based on 3D modeling and explicit time integration using the FE analysis software – LS-Dyna. Prior to the integration of the equations of motion the static problem was solved. The rotor with the blades crown was loaded with centrifugal forces, corresponding to rotation at the maximum frequency of $\omega = 3800$ RPM. The static problem was solved in nonlinear form, taking into account large deflections. The materials behavior was assumed to be linear-elastic for the static as well as following dynamic simulation.

Before solving the dynamics problem, the initial stresses associated with the action of centrifugal load and determined in the previous step are initialized in the blades and shaft elements. Centrifugal forces – as an external load – are excluded from the calculation, rotor and blade assemblies are assigned velocities corresponding to rotation at the maximum frequency. Thus, the rotor is brought into rotation, initialized initial stresses are balanced by forces of inertia arising in rotation. A test calculation was carried out to ensure absence of stress oscillations.

The blade-out was modeled by removing elements and nodes of one of the blades at time t = 0. Contact interaction of the blades with the casing has been taken into account. Time step for integration of equations of motion was capped constant and equal to $1.2*10^{-7}$ sec. The problem was solved at the interval of 0.128 sec. It corresponds to 8 full revolutions at maximum speed. No damping was introduced. It took about 12 hours to solve the problem on a powerful personal

computer.

When solving the problem using the approach outlined in Section 2, the developed software gets the input of reduced stiffness and mass 84x84 matrices. Integration of the equations of motion was performed using the Newmark method. The unbalance load is applied to the node corresponding to the disk center of mass. Characteristics of unbalance caused by loss of a single blade: $m \approx 7.3$ kg, $e = 610$ mm. Integration time was assumed to be the same as when solving the problem using LS-DYNA – 0.128 sec, time step was assumed constant at 10^{-4} sec. In order to improve the algorithm convergence when solving the problem in this form, small damping was introduced into the system. The damping was taken into account in accordance with the Rayleigh model. Damping equals 0.5% of the critical level at maximum rotor speed.

The problem was firstly solved without taking into account the contact interaction in a longer integration interval in order to certify the equivalence of the models used in the calculation and to check the accuracy of 3D explicit modeling. Fig. 10 compares the fan disk center of mass radial displacement obtained by different methods.

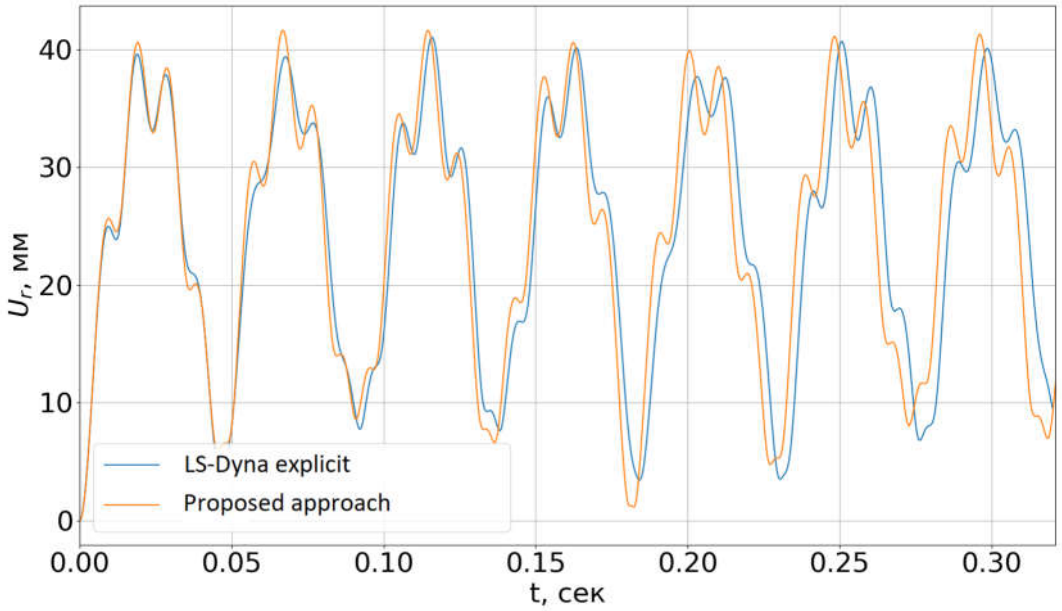

Figure 10 – Fan center of mass displacement

Solutions of the problem obtained using different models correlate well enough. Some differences may be due to the lack of considering the asymmetry of the impeller inertial characteristics when modeling using the proposed approach.

Maximum values of the forces transmitted from the rotor to the casing system through supports and contact interaction are chosen as representative results for further evaluation of the accuracy of the proposed approach to modeling the dynamics of the rotor-casing system. Calculations were performed for a number of cases with different gap values between the blades and the casing, with and without considering friction. When calculating using the proposed method in addition to differences in the gap value and friction coefficient, transferred to the developed software a different blades crown elastic characteristic was used for each of the calculated cases. The elastic characteristic was determined for different conditions in accordance with the method described in 2.2. Fig. 11 compares the calculated results in the case of no contact friction and 7-mm gap.

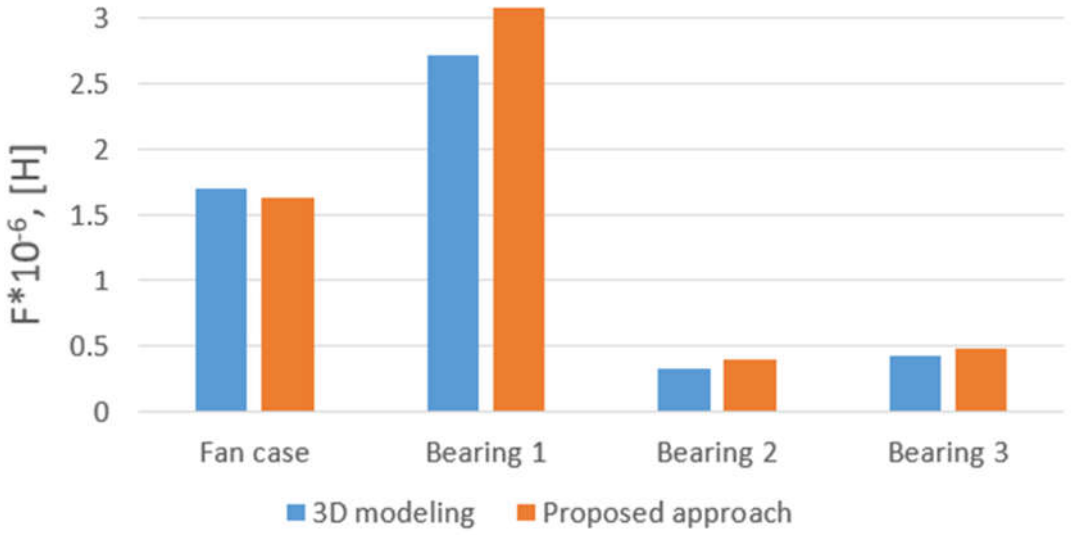

Figure 11 – Maximum fan case and bearing loads ($\Delta = 7$ mm, $\mu = 0$)

The largest differences are observed in the forces in the first support. The forces in the supports determined using the proposed approach turn out to be higher than those obtained from the results of 3D explicit simulation in LS-DYNA. The average error in determining the forces passed from the rotor to the casing system and then to the engine mounts is about 13.5%. This is an acceptable result, considering the simplifications and the difference in machine time required to solve the problem.

Comparison of forces passed from the rotor in the case of frictionless contact and 30-mm initial gap between the blades and the fan casing is shown in Fig. 12. In this case, the fan disk out of plane rotation significantly impacts the system dynamics. The average value of error in determining the forces is about 7.5%. Lack of increase in the error level indicates that the method of determining the crown elastic characteristic, taking into account disk out of plane rotation, is correct.

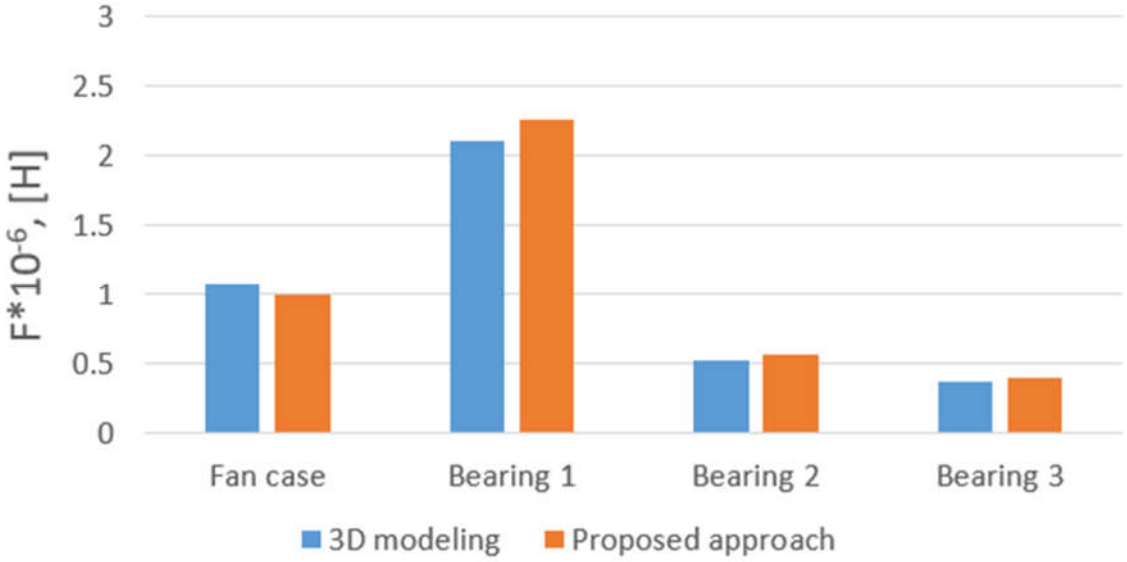

Figure 12 – Maximum fan case and bearing loads ($\Delta = 30$ mm, $\mu = 0$)

Fig. 13 shows the results of comparing maximum load values for the cases of 30-mm initial gap and taking into account the contact friction.

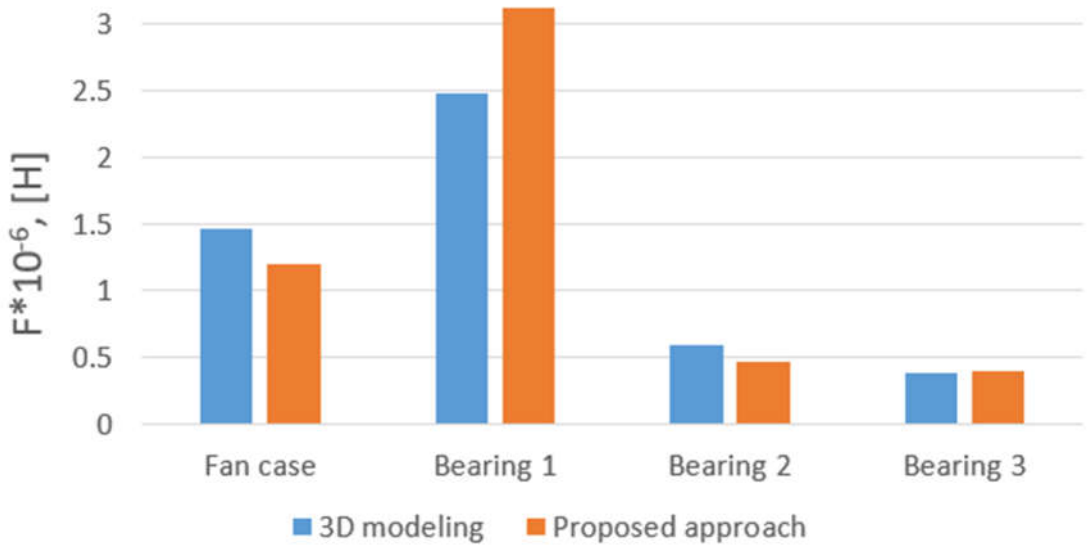

a – $\mu = 0.1$

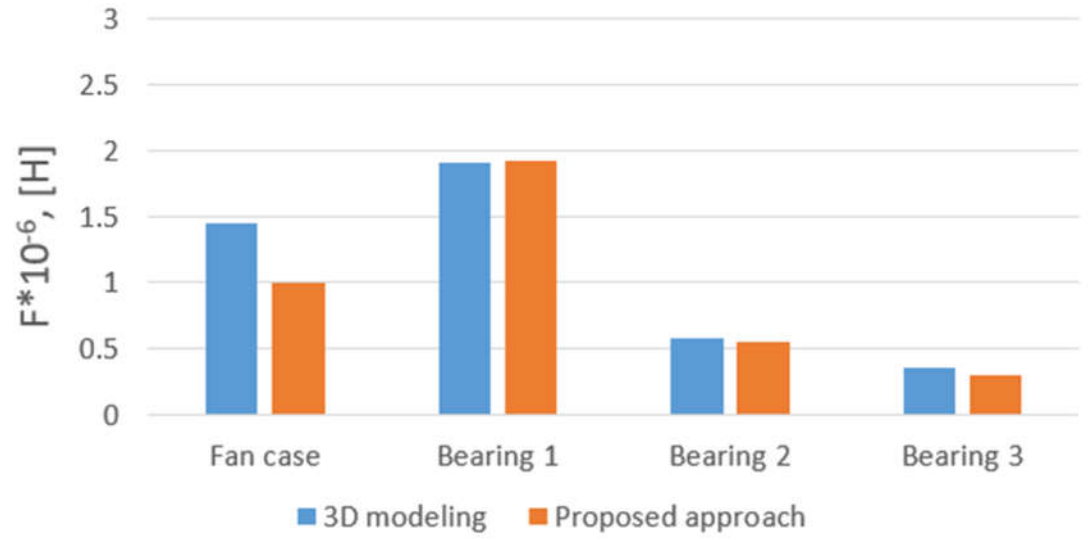

b – $\mu = 0.2$

Figure 13 – Maximum fan case and bearing loads ($\Delta = 30$ mm)

The average error in determining the loads passed from the rotor to the casing system – if calculated considering friction – increases to values of approximately 14-16%. In comparison with modeling without considering contact friction, the error in determining the loads passed to the fan casing increased. This is due to more complex behavior of blades at 3D explicit modeling with contact friction taken into account. When solving the full-size problem in LS-Dyna it is revealed that individual blades vibrate when they leave the contact and re-enter the contact zone in the subsequent moments of time. Due to the blade oscillations, conditions of repeated contacts differ, which leads to differences in the force passed to the casing and the dynamic behavior of the system as a whole. Differences in the real crown elastic characteristic, caused by the blade oscillations, are not reproduced when the characteristic is determined based on the approach outlined in Section 2.2.

5. Conclusions

The paper presents a simple and effective approach to modeling the rotor-casing system dynamics of an aircraft engine in case of fan blade-out. The proposed method allows to take into account sudden unbalance of the LP rotor in the case of FBO, the rotor speed changes due to the rotor-casing contact and the aerodynamic forces, the passage of the resonant mode by the system when the rotor decelerates. Interaction of the broken blade with the casing and trailing blades is not considered.

Special attention is paid to simulating the rotor-casing interaction through the blades crown. The paper suggests the approach to determine blades crown compliance, allowing to take into account the possibility of bladed disk out of plane rotation and also the contact friction. The influence of those factors on the crown compliance is evaluated. It was determined that the crown stiffness decreased when taking into account the disk out of plane rotation. The decrease was tied to changes in contact conditions: without considering out of plane rotation blade and casing contact occurs along the entire upper edge, when the turn is taken into account – only along the front part of the upper edge. Depending on the contact friction coefficient the crown compliance can both go up and down, which is associated with changes in the deformed configuration of the blade while compressed against the casing with different friction coefficients.

In order to assess the accuracy of the results obtained by simulation using the proposed approach, a series of calculations was performed to determine the rotor-casing system response to the sudden unbalance. Three-dimensional calculations were carried out with detailed consideration of the contact interaction by explicit modeling in LS-Dyna and on the basis of the developed method. Different blades-casing gap values, as well as different contact friction coefficients were considered. The maximum load transmitted from the rotor to the fan casing and supports are chosen as the main results for comparison.

The average error in determining the maximum loads passed from the rotor was about 8-16%, depending on the simulation case. The error is greater for the cases of contact interaction when friction is taken into account. The main source of error is a significantly simplified contact interaction modeling, in particular, not taking into account excitation of blades' vibrations at buckling or when leaving and re-entering the contact. The obtained error value is considered to be acceptable taking into account the difference in computing time needed to solve the problem. The suggested approach can be used for the initial estimation of the maximum loads on the engine components at fan blade-out.

Further work will be directed to the refinement of the rotor-casing interaction model and taking into account the casing compliance.

6. Copyright Statement

References

[1] Federal Aviation Administration. *Regulations F. A. Part 33 Airworthiness Standards: Aircraft Engines,* (Washington DC) p 59, 1993

[2] European Aviation Safety Agency. *Certification Specifications and Acceptable Means of Compliance for Engines (CS-E) Amendment 4* p 211, 2015

[3] Shmotin Y, Gabov D, Ryabov A, Kukanov S and Rechkin V. Numerical analysis of aircraft engine fan blade-out. *Proc 42nd AIAA/ASME/SAE/ASEE Joint Propulsion Conference & Exhibit,* Sacramento CA, pp 1-8, 2006

[4] Jain R. Prediction of transient loads and perforation of engine casing during blade-off event of fan rotor assembly. *Proc IMPLAST 2010*, pp 1-10, 2010.

[5] Carney K S, Lawrence C and Carney D V. Aircraft engine blade-out dynamics. *Proc Seventh international LS-DYNA users conference*, Livermore CA, USA: Livermore Software Technology Corporation, pp 14-17, 2002.

[6] Husband J B. Developing an efficient FEM structural simulation of a fan blade off test in a turbofan jet engine. Diss. University of Saskatchewan, 2007.

[7] Sinha S K and Dorbala S. Dynamic loads in the fan containment structure of a turbofan engine. *Journal of Aerospace Engineering*, Vol. 22(3), pp 260-269, 2009

[8] Sengoz K., S. Kan, A. Eskandarian. Development of a Generic Gas-Turbine Engine Fan Blade-Out Full-Fan Rig Model. *The George Washington FHWA/NHTSA National Crash Analysis Center, Washington, DC,* 2015.

[9] Genta G and Delprete C. Acceleration through critical speeds of an anisotropic, non-linear, torsionally stiff rotor with many degrees of freedom. *Journal of Sound and vibration*, Vol 180(3), pp 369-386, 1995.

[10] Hibner D H and Buono D F. Experimental study of transient dynamics of a flexible rotor, NASA, Washington D.C., 1976.

[11] Wang C, Zhang D, Ma Y, Liang Z and Hong J. Theoretical and experimental investigation on the sudden unbalance and rub-impact in rotor system caused by blade off. *Mechanical Systems and Signal Processing*, Vol 76, pp 111-135, 2016.

[12] Yu P, Zhang D, Ma Y and Hong J. Dynamic modeling and vibration characteristics analysis of the aero-engine dual-rotor system with Fan blade out. *Mechanical Systems and Signal Processing*, Vol 106, pp 158-175, 2018.

[13] Ma H, Yin F, Guo Y, Tai X and Wen B. A review on dynamic characteristics of blade-casing rubbing. *Nonlinear Dynamics*, Vol 84(2), pp 437–472, 2016

[14] Heidari M, Carlson D, Sinha S, Sadeghi R, Heydari C, Bayoumi H and Son Jin. An efficient multi-disciplinary simulation of engine fan-blade out event using MD Nastran. *Proc 49th AIAA/ASME/ASCE/AHS/ASC Structures, Structural Dynamics, and Materials Conference, 16th AIAA/ASME/AHS Adaptive Structures Conference, 10th AIAA Non-Deterministic Approaches Conference, 9th AIAA Gossamer Spacecraft Forum, 4th AIAA Multidisciplinary Design Optimization Specialists Conference*, Schaumburg, IL, 2008.

[15] Weng Y and Lipeng Z. An Explicit-Implicit Time Integration Approach for Finite Element Evaluation of Engine Load Following an FBO Event. *Proc ASME Turbo Expo 2017: Turbomachinery Technical Conference and Exposition*, Charlotte, NC, GT2017-64636, pp 1-8, 2017.

[16] Myasnikov V Y and Ivanov I I. Method of engine structural frame vibrations analysis during fan blade-out. *IOP Conference Series: Materials Science and Engineering*, Vol 489(1), pp 1-8, 2019.

[17] Bathe K J. *Finite element procedures,* New Jersey: Prentice Hall, 2006